عدد خاص
بالمؤتمر الليبي الدولي للعلوم التطبيقية
و الهندسية
27-28- سبتمبر 2022

Relationships Between Microstructure and Pitting Corrosion For ADI in Chloride media

WafaYousef Eljaafari[1], Salem Musa[2], Mohamed Alaalam[3].
1-The Higher technical center for training and production, Tripoli-Libya.
2- University of Tripoli, Faculty of Engineering, Metallurgical & Materials Engineering Dept.
3-Libyan academy ,Tripoli.

Abstract
Austempered ductile iron (ADI) has complex microstructure containing a multiphase matrix called "austferite". The corrosion resistance of ADI is related to its microstructure which is determined by heat treatment parameters (austempering temperature, austempering time, austenitizing temperature and austenitizingtime). In this work, the electrochemical behavior and corrosion resistance of ADI have been investigated by electrochemical and non-electrochemical tests in chloride media. Particular attention has been paid to the influence of austenitization time (30,60,120,180,360 and 390) on the microstructure and their influence on ADI corrosion behavior. It has been shown that ADI austenitization at 850^0C for different times and austempered at 360^0C for three hours has generally ausferritic microstructure. Retained austenite ranges between 20% to 40%. Hardness increasesd with increasing austenitization time. Electrochemical and non-electrochemical testing in chloride solution showed general corrosion and pitting corrosion was observed in one sample in the electrochemical test.
Key Words: ADI, NaCl solution, pitting corrosion, microstructure of ADI, Corrosion tests.

الملخص
حديد الزهر المستمبر له تركيبة مجهرية معقدة تحتوي على عدة أطوار تسمى أوسفرايت . مقاومة التآكل لحديد الزهر المستمبر ترتبط بالتركيبة المجهرية وتتحدد بعوامل المعالجة الحرارية (زمن الأستنة ,درجة حرارة الأستنة, زمن الأيزوتمبر , درجة حرارة الأيزوتمبر) . في هذا العمل , السلوك الكهروكيميائي ومقاومة التآكل لحديد الزهر المستمبر تم التحقق منهم بواسطة الطرق الكيميائية والغير كيميائية في الوسط الملحي.
وقد تبين أن تأثير زمن الأستنة عند درجة حرارة 850 م^0 لأزمنة مختلفة ومستمبرد عند درجة 360م ^{0} لثلاثة ساعات تحتوي في العموم على تركيبة مجهرية أوسفرايتيه. يتراوح مدى الأوستنايت المتبقي ما بين 20– 40%. قيمة الصلادة تزداد بزيادة زمن الأستنة . أظهرت الإختبارات الكهروكيميائية واللاكهروكيميائية في المحلول الملحي تآكل عام بينما أظهرت عينة واحدة تآكل نقري في الإختبار الكهروكيميائي.

1. Introduction

Austempered ductile iron is one of the results of the most significant development in cast iron technology since discovery of ductile iron. Austempering heat treatment has generated a new family of ductile iron with improved mechanical properties, and with strength levels double those of other ductile iron grades and the same level of ductility and with comparable to some wrought iron. ADI has complex microstructure called "ausferrite". The corrosion resistance of ADI is related to its microstructure which is determined by heat treatment parameters [1]. ADI is a ductile iron that has been heat treated by the

austempering process to make it tougher than regular ductile iron of half the strength. The microstructure of ADI strongly depends on austempering temperature and time. Austempering to high temperatures promotes the formation of relatively thick ferrite laths in an austenite matrix enriched in carbon. When austempering is carried out at lower temperatures, thinner needles of acicular ferrite result. If austempering time is very short, the degree of advance of the transformation is less than 100% and a percentage of untransformed austenite remains, that could transform to martensite during cooling also if austempering time is too long, as the second stage of transformation begins, carbon precipitates in the form of carbides [2-3]. The influence of austenitizing condition on the mechanical properties of the alloy under investigation were studied[4]. However, no corrosion data were available in the literature for this particular alloy. Therefore, the present work, will focus on investigating the relationships between microstructure and pitting corrosion of ADI alloy in chloride media. This will be achieved by means of conventional weight loss method according to international standards and by electrochemical measurements techniques. Corrosion behavior of a material is quantitatively expressed in terms of corrosion rate [5]. Corrosion rate can be calculation by using the following equation:

Corrosion rate (mpy) = KW/DAT ……1.

Where W= Weight loss (g). K= a constant depended on unites were used .D= Density of sample (g/ cm^3). A= Area of sample (cm^2). T= Exposure time (days).

2. Experimental Work

Chemical analysis of the as received material was conducted using Spark emission spectro-meter. The composition in wt. % is given in table 1.

Table 1: Chemical Composition of the alloy used in this work.

Element	C	Si	Mn	S	P	Mg	Cu	Ni	Fe
%	3.3	2.6	0.35	0.008	0.01	0.04	1.6	1.6	Balance

The received six austempered ductile iron samples were subjected to different austenitizing times (30, 60, 120, 180, 360 and 390) minutes at constant austenitizing temperature of 850^0C, then austempered at 360^0C for three hours. Teste samples were given A_1, A_2, A_3, A_4, A_5 and A_6 symbols respectively**.** Metallographic samples were ground by the abrasion of the specimen surface against water lubricated abrasive wheels (silicon carbide papers changing from "120 to 1200 –girt emery paper"). After grinding, the polishing process was done by the use of the rotary disk with diamond paste. Then, the etching operation was done with the 2% nital solution (2% nitric acid solution in 98% ethyl alcohol). Microstructural examination was carried out using Nikon optical microscope equipped with digital camera type (Am Scope MU800). Six samples designated as (A_1, A_2, A_3, A_4, A_5, and A_6) to be immersed inNaCl. The method for specimen preparation is done in accordance to ASTMG1. The investigated samples surface preparations were carried out by grinding machine using silicon carbide paper to 600 girt finishes. When the required surface preparation quality was achieved, the samples were rinsed thoroughly with distilled water, and dried by an air stream.

In order to provide an electrical contact between the testing specimens (the working electrodes) and the voltage source (the potentiostat), an insulated copper wire was soldered to one side of each specimen. The specimens were then cold mounted using two-component (Acryfix) epoxy resins and prior to each electrochemical test, the exposed surfaces of the coupons were sequentially wet ground using a sequence of silicon carbide paper to 600 girt finished by using the grinding machine. When the required surface preparation quality was achieved, the electrodes were rinsed thoroughly with distilled water, and dried by an air stream.

2.1 Corrosion test

2.1.1 Immersion test

In order to determine corrosion rate using weight loss method, the immersion test was conducted in accordance to ASTM G 67. The initial weight (W_1) was determined before immersion using sensitive Scaltec microbalance with four-digit sensitivity. Before immersion test the specimen were ultrasonically cleaned in ethanol, dried and then immersed in 1M and 0.5M "NaCl " solution for 5 and 35 days respectively as shown in figures (1,2) and the final weight was taken (W_2).

Figure 1: Weight loss test for samples immersed .in 1M NaCl

Figure 2: Weight loss test for 0.5M NaCl

The corrosion rates of the corroded samples immersed in this media (NaCl) was determined using the standard mathematical relationship**.**

2.1.2 Electrochemical Testing

The electrochemical tests were performed at the corrosion laboratory of the Libyan Petroleum Institute, Tripoli, using a computer controlled ASM interface model Gill 12. An overview of the electrochemical testing device is shown in Figures (3 & 4) for each experiment, a 300ml of the testing solution (0.5M NaCl) was poured into the corrosion cell at room temperature, which was connected to the electrochemical interface, and by the aid of version 5 ASM sequencer and core running software, the potential and current density were recorded and converted into a graphic relation. In order to obtain reproducible results, the testing coupons were left at their free corrosion potentials for 15 minutes prior to each potential scan.

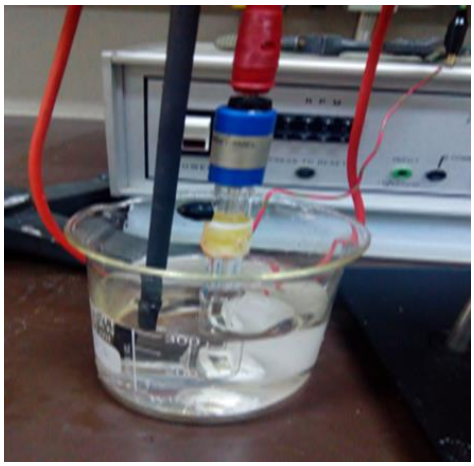

Figure 3: Cell Setup

Figure 4: Electrochemical testing device used in the presentwork

2.1.2.1 Potential Polarization (PP)

For anodic polarization experiments, the potential scan was started at -400mV relative to the sample free corrosion potential with a scan rate of 1mv/ sec and terminated when the current density reached 1mA/cm^2. The test was repeated after surface polishing.

2.1.2.2 Linear polarization resistance (LPR)

For linear polarization experiments, the potential scan was started at -10mV relative to the sample free corrosion potential with a scan rate of 1mv/sec and terminated when the current density reached 1mA/cm^2.

2.1.2.3 Tafel constant

For Tafel constant experiments, the potential scan was started at -50mV relative to the sample free corrosion potential with a scan rate of 1mv/ sec and terminated when the current density reached 1mA/cm^2.

2.3. Surface Morphology

Scanning electron microscope (SEM) analysis was performed with a LEO1430VP microscope to obtain information regarding the morphology and types of corrosion.

2.4 x -ray diffraction

The X-ray diffraction was used for phase identification that appeared in the microstructure of the ADI. The x-ray diffraction patterns were taken using computerized x-ray diffractometer (Model: pw 1800 of M/s Philips NV, Holland). All x-ray diffractograms were taken by (Cu-Kα) radiation (wavelength, $\lambda = 1.5406A^0$). A tube voltage of 40Kv, a tube current of 30mA, and a step time of one second were used.

2.5 Hardness measurement

Hardness testing machine was used to measure the hardness property . The final hardness values were measured by taking the average of the five hardness values.

3.0 Result and Discussions:

3.1 Microstructural investigation

The effect of austenitization time for (30, 60, 120, 180, 360, and 390 minutes) at austenization temperature of 850^{0}C for sample designated as A_1, A_2, A_3, A_4, A_5 & A_6 on the microstructure

has been studied by optical microscopy and x – ray diffraction. The resultant microstructures consist of ferrite (α) needle in a stabilized high carbon austenite matrix a structure as ausferite, nodular graphite and oxide inclusion. As the time of austenitization is increased to 180, 360 and 390 min, the acicular ferrite and retained austenite get distributed more uniformly due to homogeneous carbon content of austenite in the matrix. The shape of the ferrite needles become more elongated, narrow and interlocked; the graphite nodules were unaffected; this can be revealed in the microstructure of the tested samples as shown in figure 5.

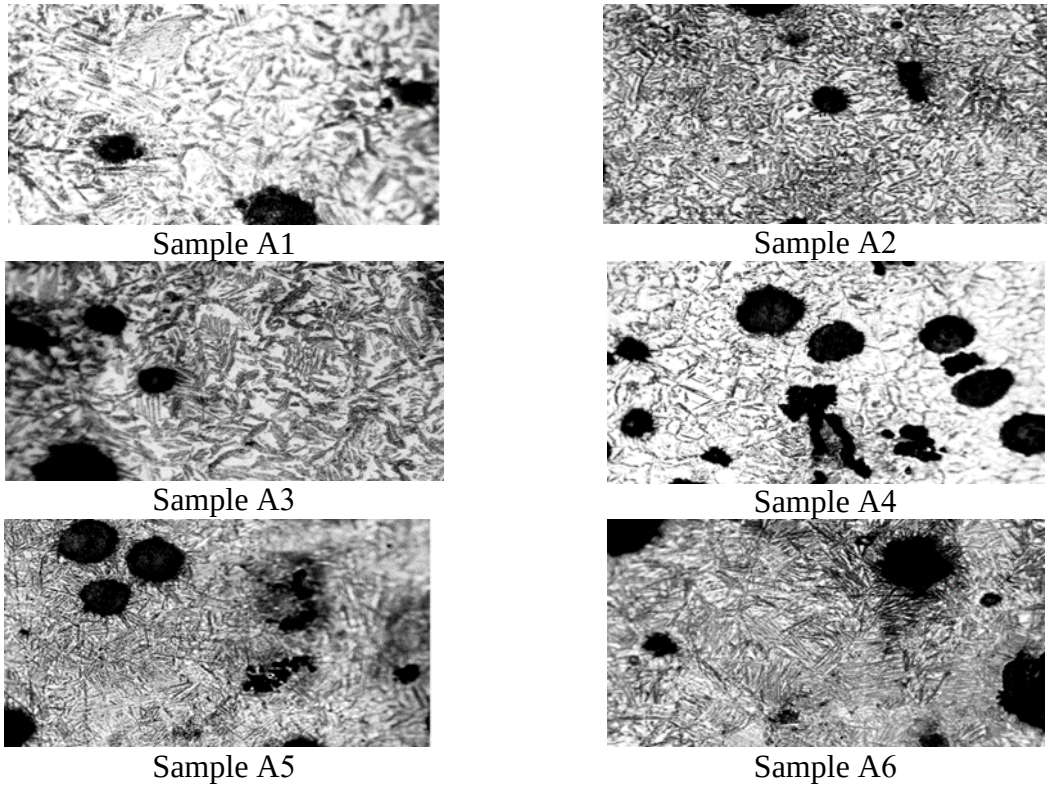

Figure 5: Microstructure of ADI samples.

On comparing the microstructures between samples (A_1) and (A_2) as well as (A_5) and (A_6), From figure 5, it is noted that A_1 showed no significant microstructure difference. The difference appeared as the austenitization time is increased by one hour. This can be observed clearly on comparing the microstructures of samples A_2, A_3, A_4 and A_5. The result of x-ray diffraction profiles obtained from A_1, A_2, A_3, A_4 & A_6 were analyzed on a computer to obtain the peak positions and the integrated of intensity of (111), (220) and (220) peaks of austenite and (110) and (211) peaks of ferrite. Each set of diffraction patterns were analyzed using computer program and Sakahat Virtual lab. Formulas to determine the 2 Θ value at each peak and the integrated intensity under the peaks were used to calculate the percentage of retained austenite and was found to fall between 20 to 40 % that is based on ASTM method [6]. Carbon contents of retained austenite phases were calculated using computer program and their results

were found to be in a good agreement with it. This finding was agreed with the work done by J. Abderahim [7]. Which show has been found that, the value of retained austenite and carbon content for it alloy used investigation at austenitization 900^0C and 1000^0C for 3hours were (27.81% , 35.63% , 1.6990 %and 1.70%) respectively.

3.2 The immersion test

Figure. 6 showed that A_6 samples gives the lowest corrosion rate , while A_1 gives the highest Corrosion of immersion test samples in 1M NaCl.

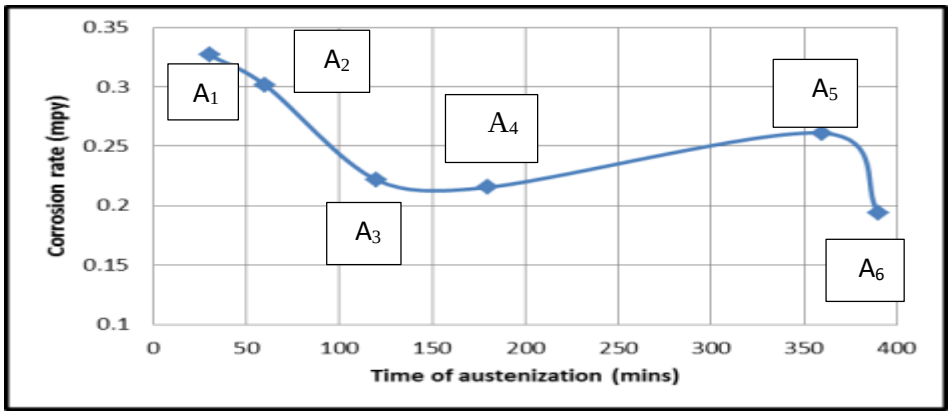

Figure 6: Corrosion rate vs austenitization time for ADI austenitization at 850^0C, austempered at 360^0C for 3hrs. and immersed in 1MNaCl.

However, figure.7 indicated that A_6 sample gives lowest corrosion rate, where A_4 gives the highest corrosion rate of 0.5 M NaCl immersion test.

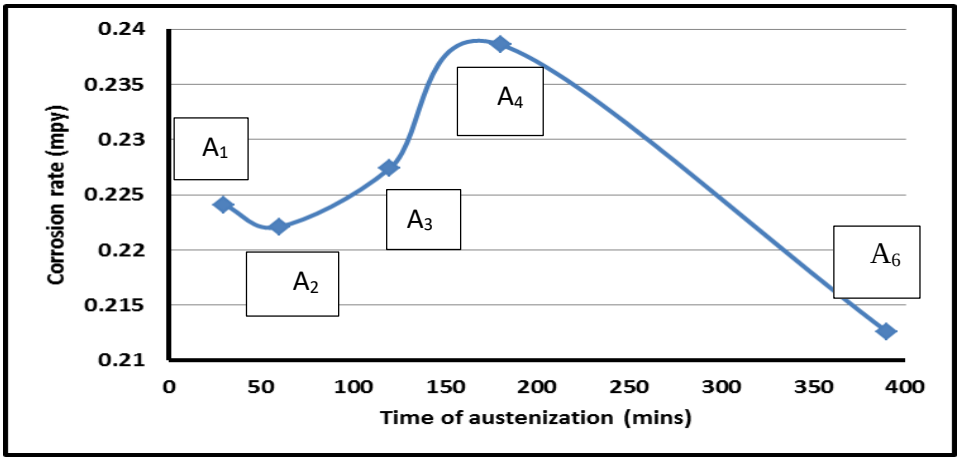

Figure 7: Corrosion rate vs austenitization time for ADI austenitized at 850^0C, austempered at 360^0C for 3hrs. and immersed in 0.5 M NaCl.

Generally, the corrosion rate results showed the same trend. However, corrosion rate obtained from samples immersed 1M were higher than that obtained from samples immersed in 0.5M. This attributed to the higher concentration of chloride ions in 1MNaCl solution which led to

high speed of electron transfer and metal dissolution of iron in an electrolyte. These finding agree with work by M.S.Ali [8] ,Reported the value of corrosion rate for ductile cast iron ,austenitization temperature 850^{0}C for 90minutes immersed in 3.5% NaCl for 1, 7, 14 and 28 days were 0.14, 0.187, 0.34 and 0.67 mm / year (mpy).

3.3: The electrochemical test

IN order to investigate corrosion behavior of the austempered ductile iron a potential technique was performed to the A_1,A_2,A_3,A_4,and A_6 samples that were austenized at 850 ^{o}C for (30,60,120,180 and 390 minutes), austempered at 360 ^{O}C for three hours. The electrochemical test was performed in 0.5M NaCl solution. A linear polarization test was performed in order to calculate the corrosion rate.

3.3.1 Potentiodynamic Polarization

Potentiodynamic polarization technique was used to study the general behavior of the ADI samples in the 0.5 solution. The testing samples were left at their free corrosion potentials for 15 minutes prior to each potential scan. The scan was then performed from cathodic potential to anodic potential with scan rate of 30 mv/min. This took 50 minutes to complete. Figures 8 shows the polarization curves for samples designated as A_1 (Black color), A_2 (Green color), A_3 (Blue color), A_4 (Red color) and A_6 (Yellow color).

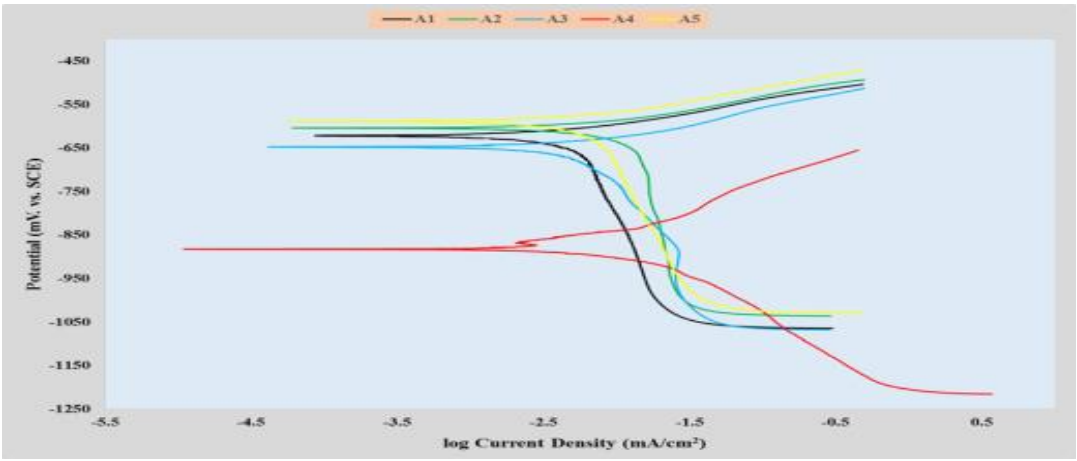

Figure 8: The Potentiodynamic polarization curves for tested samples in 0.5M NaCl.

Figure 8 Showed that A_1, A_2, A_3, A_6 samples suffered from general corrosion while A_4 showed pitting corrosion at corrosion potential of about -850 SCE. This could be attributed to some irregularity at its surface. A_4 sample have the lowest active corrosion potential. Global electrochemical measurements suggest that the ADI samples with the ausferritic microstructure (austenitized at different times and austempered at 360^{0}C) are less prone to pitting corrosion. The changes observed in the corrosion resistance was related to the microstructural modifications induced by austenitization times which results to greater coarsening of the austenite grains and broad ferrite needles as the austenitization time decreased. It is well known that grain boundaries are defects that could be more sensitive to corrosion. Hence, greater coarsening produces less ferrite/austenite interfaces, leading to the better electrochemical behavior of ADI in sodium chloride solution.

3.3.2 Linear Polarization Resistance (LPR)

The corrosion potentials and the corresponding current densities were recorded every 24 hours. Results values were presented in Table 2.

Table 2: Corrosion potential & current density for tested samples.

Sample Symbol	A_1	A_2	A_3	A_4	A_6
Corrosion Potential (mv)	-734.67	-729.96	-740.24	-734.22	-727.37
Current Density ($mAcm^2$)	0.005881	0.005304	0.005934	0.007952	0.006598

The corrosion potential is used as an overvoltage reference point and a straight line was obtained within 10mV more active and more noble from the corrosion potential. The slope of this linear polarization curve is the polarization resistance (Rp) as shown in figure 9, and from the beta values shown in Table 3.

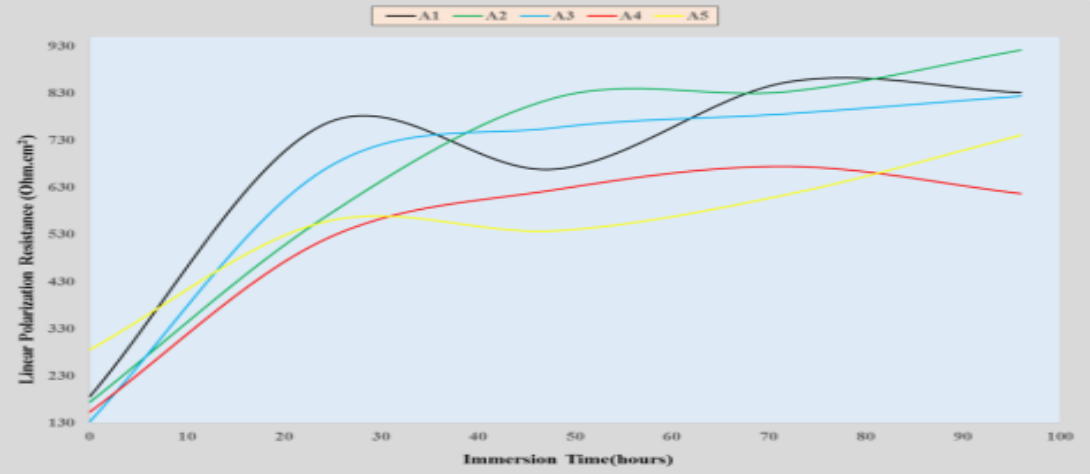

Figure 9: The result of linear polarization resistance.

Table 3: Shows the value of Tafel constant.

Name of constant	Anodic Tafel βa	Cathodic Tafel βc
Value of constant	25.882	25.955

Corrosion rate was calculated by using equation.1 as shown in Table. 4.

Table 4: Corrosion rate of tested samples obtained by linear polarization technique.

Sample Symbol	A_1	A_2	A_3	A_4	A_6
Corrosion rate (mils/ year)	5.2358	4.5424	5.0810	6.7852	5.6469

From Table.4, it is clearly indicated that A_4 gives the highest value of corrosion rate while A_2 gives least value.as shown figure 10.

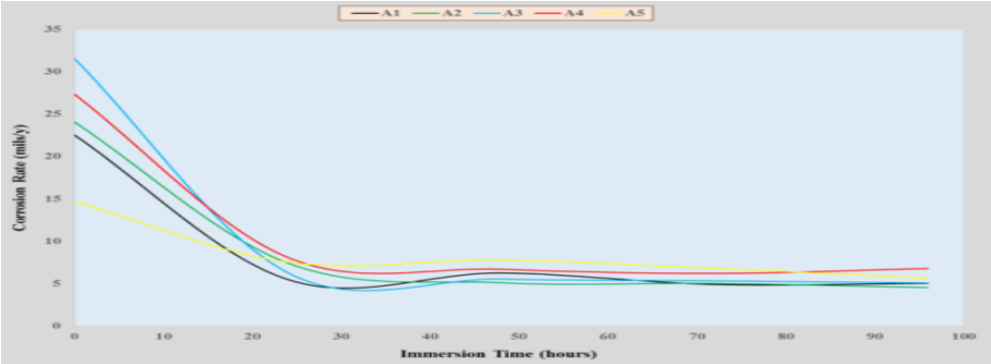

Figure 10: Shows the corrosion rate for each sample as a result.

Figure 11 Shows the surfaces of the tested samples after linear polarization test by using a normal Camera. Surfaces were suffered from general corrosion except the surface of A_4 sample was suffered from pitting corrosion. This was confirmed by optical microscope as shown in figure 12.

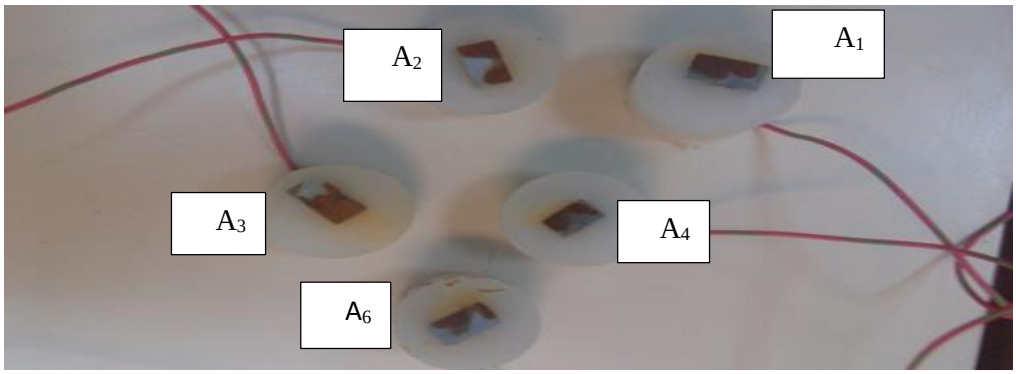

Figure 11: Photograph the surface after LPR test

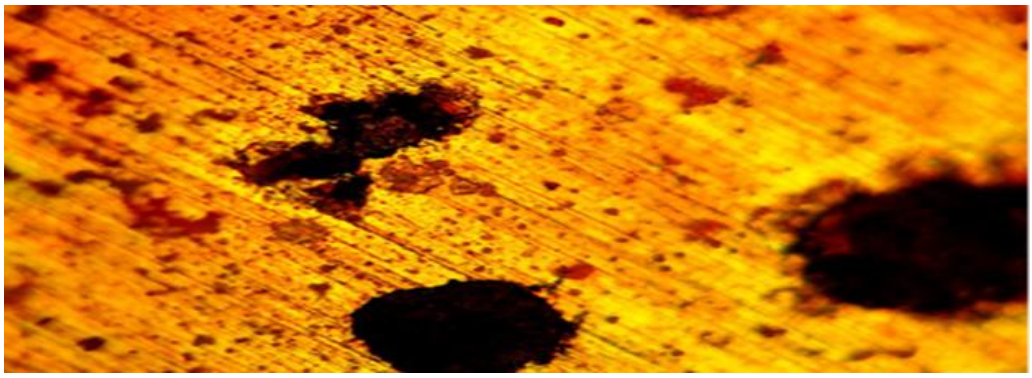

Figure 12: Surface microstructure of A_4 sample using optical microscope.

The results of corrosion rates obtained from the electrochemical and non -electrochemical test were found different. These finding agree with work done by M.S .Ali [9], it has been that the value of corrosion rate for ductile cast iron, austenitization temperature 850^0C for 90 minutes in 3.5% NaCl was 7.99 mpy.

4.4 Surface morphology after LPR tests using (SEM)

Figure 13 represents the scanning electron microscope (SEM) micrographs of the surface morphology after the potentiodynamic polarization. From the figure, all samples show general corrosion on their surfaces except (A_4) sample showed pitting.

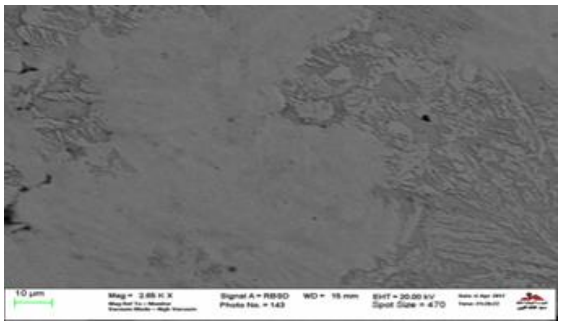

A1 shows general corrosion in a little region of the surface and another area doesnot present any corrosion

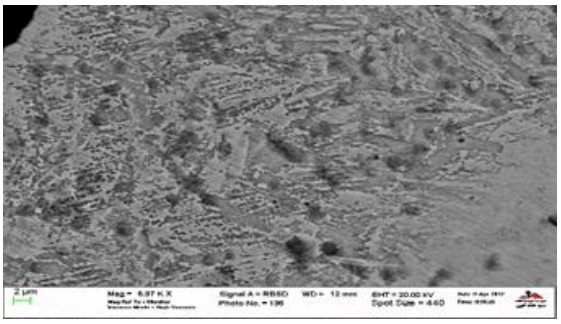

A2 shows general corrosion

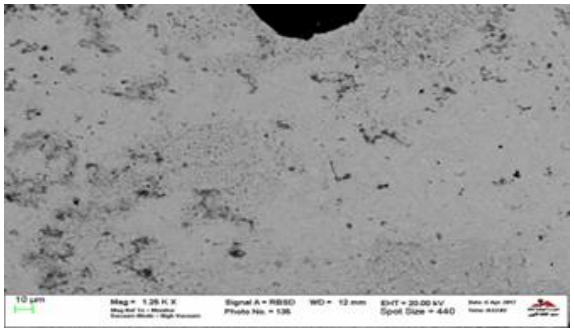

A3 shows general corrosion

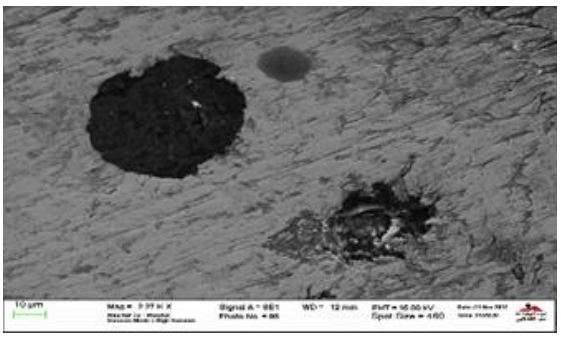

A4 shows pitting corrosion

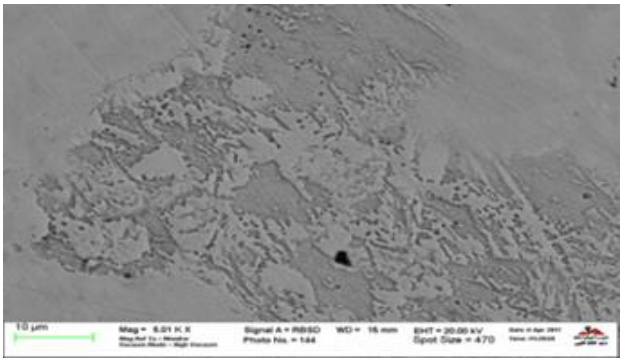

A6 shows general corrosion

Figure13: The scanning electron microscope (SEM) micrographs of the surface morphology after the potentiodynamic polarization

4.5 The result of hardness test

Hardness measurement of the investigated ADI alloy samples were performed and the results were presented in figure14. The hardness is increased as the austenitization time is increased.

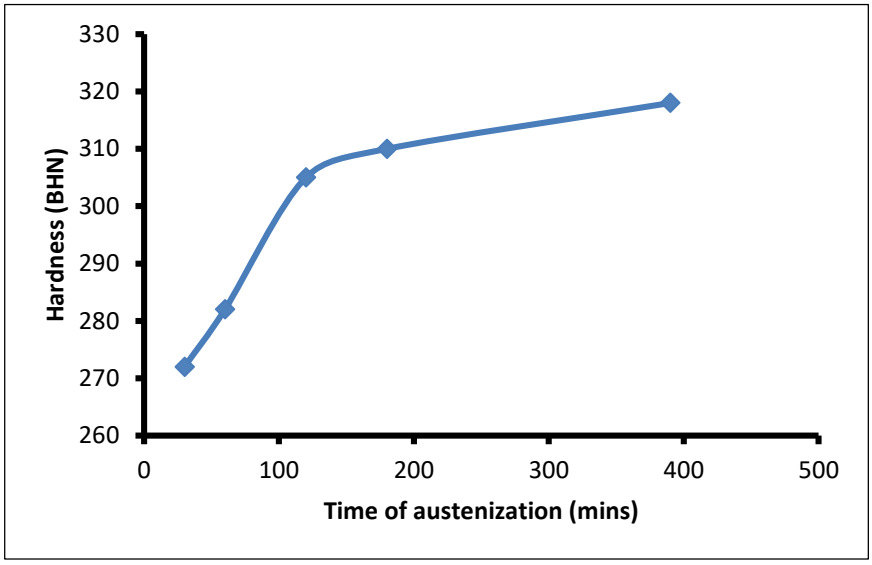

Figure14: The effect of the austenitizion time on the hardness measurement

5.1 Summary and Conclusions

This research was designed to investigate the relationships between microstructure and pitting corrosion and has led to the following conclusions:

1- Austenitization time for cycle heat treatment ADI has slight effect on microstructure and corrosion behavior for1.6Cu-1.6Ni alloy.

2- Corrosion rate in chloride media depends on the type of the microstructure.

3- Hardness of ADI increases with increasing time of austenitization.

References

[1] A.Sinlah, “Machining austempered ductile iron”, Society of manufacturing engineering, vol.128. No,5, 2002,pp.125.

[2] S.K. Sahoo," A study of machinability in milling of austempered ductile iron ADI 900, ADI 1050, and ADI 1200 with carbide tools, " 2014,pp.43.

[3] M.D.Corobbo,and Sergio Arias " Evolution of impact and fatigue properties of ADI," National institute of technology, 2012,pp.14.

[4] M. Grech, Mohamed Alaalam and M. Delia. Effect of Austenitising Conditions on the Impact Properties of an Alloyed Austempered Ductile Iron of Initially Ferritic Matrix Structure, ASM Journal of Materials Engineering and Performance, USA, Volume 7 No 2, April 1998.

[5] M. Pooja, V. Vijeesh, A. O. Surendranathan, K. R. Udupa, K. G. Samuel, "International Journal of Engineering Science and Technology ", Vol.8, No.3, 2016, pp.7-12.
[6] M.Pourbaix,Atias of Electrochemical Equilibria in Aqueous solution,Second English,Edition 1974 by National Association of corrosion engineers, Houston,Taxes,USA, Chapter IV,pp.452-455.
[7] J.Abdulrahim," Effects of austenitizing conditions on the volume fraction and the carbon content of austenite for alloyed ADI of initially ferritic matrix structure ", 2007,pp.25.
[8] Ali Hubi Haleem., Assist. Lect. Firas Jabar, Assist. Lect Newal Mohammed. "Corrosion behavior of cast iron in different aqueous salt solution", 2010, pp.1.